



## Magnetic fields of red giants and supergiants: a review of spectropolarimetric observations

S. Plachinda<sup>1</sup>, V. Butkovskaya<sup>1</sup>, D. Shulyak<sup>2</sup>, N. Pankov<sup>1</sup>, V. Tsymbal<sup>3</sup>

<sup>1</sup> Crimean Astrophysical Observatory, Nauchny 298409  
e-mail: [psi@craocrimea.ru](mailto:psi@craocrimea.ru)

<sup>2</sup> Instituto de Astrofísica de Andalucía – CSIC, Glorieta de la Astronomía s/n, Granada 18008, Spain

<sup>3</sup> Institute of Astronomy of the Russian Academy of Sciences, Pyatnitskaya str. 48, Moscow 119017, Russia

Submitted on October 12, 2021

### ABSTRACT

Magnetic fields have reliably been detected so far in many classes of stars with convective envelopes, from young T Tauri stars to supergiants. We present an overview of the results obtained with high-precision spectropolarimetric observations of selected single F0–M0 giants and supergiants. The measurements of the magnetic field in these objects were started in 1989 at the 2.6-meter ZTSh telescope of the Crimean Astrophysical Observatory. To date, weak magnetic fields have been recorded in nearly four dozen slowly rotating red giants. The longitudinal component of the field in several cases reaches a few tens of gauss. A spectropolarimetric survey of red supergiants includes three dozen objects. The magnetic field was detected in a dozen of them. For one of these targets,  $\epsilon$  Gem, the magnetic field up to 10 G was reported. Since the magnetic field is frozen into the plasma, it is expected that the magnetic field of giants and supergiants should not exceed one gauss because stars have increased in size after the main sequence. Therefore, the main conclusion from the results of spectropolarimetric surveys of giants and supergiants with convective envelopes is that the most probable mechanism for the generation and amplification of the magnetic field in these objects is the dynamo action.

**Key words:** stars: late-type, stars: magnetic fields, stars: giants, stars: supergiants

### 1 Spectropolarimetric measurements of the stellar magnetic field: some initial considerations

Obtaining reliable data on the strength and geometry of the global stellar magnetic field, as well as on the magnetic field in active regions, requires several mandatory steps (Plachinda et al., 2019, 2021).

1. Control for the alignment of the spectropolarimeter and quality of the primary processing of observations.
2. Accurate continuum normalization of polarized spectra, because the function chosen to represent local continuum should not distort the distribution of polarization along the spectral line profiles.
3. Control for the instrumental outliers that might be present in polarization spectra.
4. Control for the statistical properties of the observed spectra and the measured magnetic field using the Monte Carlo method (any CCD matrix is an almost ideal sample of the normal distribution of the accumulated signal).
5. Choice of the optimal method for calculations of the Stokes profiles (LSD (Donati et al., 1997) or SL and COALA (Butkovskaya and Plachinda, 2007) and

(Plachinda et al., 2019). For more detailed descriptions of these methods see below.).

The LSD method (Least Square Deconvolution) uses a full available set of spectral lines and their blends to derive the weighted pseudo-mean Stokes profiles. This allows one to increase the signal-to-noise ratio and detect weak magnetic fields up to one-tenth of a gauss. Though the LSD method has been providing spectacular results for many years, it still has certain limitations and thus cannot be applied in a number of astrophysical problems. These limitations come from the assumptions implemented in the method:

- 1) all line profiles have similar shapes;
- 2) in the initial version of LSD, a profile of the blend was represented by a linear sum of components (Donati et al., 1997);
- 3) physical conditions and the geometry of the magnetic field of a star should be homogeneous on the surface and with the depth in the atmosphere.

According to computations, these assumptions are too rough in solving a number of problems and lead to an artificial mismatch between model LSD and observed spectra. In addition, the multiline technique works only with weak lines and is

suitable for measuring relatively weak fields ( $B \lesssim 1500$  G) (see, e.g., Fig. 6 in [Ramírez Vélez, 2020](#)).

The main advantage of the LSD method over the SL method is as follows. Because LSD uses blends (see a new approach in [Sennhauser et al., 2009](#)) along with unblended spectral lines, this allows one to retrieve a high signal-to-noise ratio for the Stokes parameters. Unlike LSD, the SL method (Single Line; the center of gravity method for individual spectral lines) normally uses fewer lines that are analyzed individually ([Plachinda and Tarasova, 1999](#); [Plachinda, 2004, 2014](#); [Butkovskaya and Plachinda, 2007](#)). This allows one to search for, e.g., inhomogeneity of physical conditions on a star ([Plachinda et al., 2019](#)).

To calculate the longitudinal field component according to the LSD method, the following formula is used ([Borra and Vaughan, 1977](#)):

$$B_l = 714.53 \times 10^4 \frac{\int \Delta v V_c(v) dv}{\bar{g} \lambda \int [1 - r(v)] dv}, \quad (1)$$

where, for the weighted mean profiles,  $\Delta v$  is the value ( $\Delta \lambda_B = 4.6685 \times 10^{-13} \bar{g} \lambda^2 B_l$  (Å)) of energy level splitting of an atom in the magnetic field in velocity units (km/s);  $\bar{g}$  is the mean Lande factor of magnetic splitting,  $\lambda$  is the resulting wavelength and  $r(v)$  is the non-polarized contour,  $V_c$  is the normalized to the continuum  $V$  Stokes parameter. Here  $2V_c(v) = r_l(v) - r_r(v)$ , where  $r_l(v)$  is the left circularly polarized contour and  $r_r(v)$  is the right circularly polarized contour of the spectral line.

According to the SL method, the magnetic field calculation from individual spectral lines is performed through the formula (see, e.g., [Plachinda, 2014](#)):

$$B_l = \frac{714.53 \times 10^4}{\bar{g} \lambda} \left\{ \left( \frac{\int \Delta v (r^*(v) - r(v)) dv}{\int (r^*(v) - r(v)) dv} \right)_1 - \left( \frac{\int \Delta v (r^*(v) - r(v)) dv}{\int (r^*(v) - r(v)) dv} \right)_2 \right\}, \quad (2)$$

where  $r^*(v)$  is the limitation function of the used polarized contour part of the absorption line from the side of the continuum;  $r(v)$  is the polarized contour profile function. Indices 1 and 2 denote the number of the used two exposures for calculations.

COALA (COntour ALgorithm of the Line Approximation) is the method of normalization of polarized profiles based on the dependence of the residual intensity of the observed polarized profiles on their central residual intensity [Plachinda et al. \(2019\)](#).

## 2 First spectropolarimetric surveys

### 2.1 Giants and supergiants

The selected results of spectropolarimetric surveys of magnetic fields in stars with convective envelopes are presented below. These results allow one to conclude that the magnetic fields in these stars are generated and amplified by stellar dynamos. However, it is not known what is the exact ratio

between the relict and generated magnetic fields that contribute to the global magnetic field of a star.

The magnetic field on late-type giants was first detected using a magnetometer by [Borra et al. \(1984\)](#): for  $\alpha$  Boo (Sp K2 III)  $B_e = +3.3 \pm 0.5$  G and for  $\mu$  Gem (Sp M3 III)  $B_e = +9.1 \pm 2.0$  G.

The first spectropolarimetric surveys were performed by [Hubrig et al. \(1994\)](#), [Tarasova \(2002\)](#), [Plachinda \(2005\)](#). They measured the magnetic field in slowly rotating stars with convective envelopes from dwarfs to supergiants using the long-slit spectrograph and the polarization analyzer plus CCD as a detector. Therefore, only a short part of the spectrum having no more than two dozen of suitable spectral lines was recorded with CCD. This explains the fact why the accuracy of magnetic field measurements was only several gauss. Nevertheless, this accuracy proved to be sufficient to register statistically significant magnetic fields on the surface of the selected stars.

**Table 1.** The magnetic field in giants and supergiants

N	Object	Sp	$B_e \pm \sigma$	$B_e/\sigma$
1	$\epsilon$ Gem <sup>5)</sup>	G8 Ib	+11.1 ± 2.7	4.1
2	$\epsilon$ Peg <sup>2)</sup>	K2 Ib	-5.3 ± 0.9	5.9
3	$\epsilon$ Leo	G1 II	+49.2 ± 6.1	8.1
4	$\zeta$ Cyg	G8 II	+5.4 ± 1.7	3.2
5	$\zeta$ Hya	G9 II	-15.3 ± 2.9	5.3
6	$\eta$ Psc	G7 III	+11.4 ± 3.9	2.9
7	$\kappa$ Gem <sup>2)</sup>	G8 III	+13.0 ± 3.8	3.4
8	$\mu$ Peg <sup>2)</sup>	G8 III	-20.1 ± 3.3	6.1
9	$\epsilon$ Vir	G8 III	-10.8 ± 3.2	3.4
10	$\xi$ Her	G8 III	-28.1 ± 4.5	6.2
11	$\gamma$ Tau	K0 III	+19.8 ± 5.2	3.8
12	$\epsilon$ Cyg <sup>2)</sup>	K0 III	+9.3 ± 2.5	3.7
13	$\epsilon$ Tau	K1 III	-22.3 ± 5.4	4.1
14	$\delta$ And <sup>2)</sup>	K3 III	+8.5 ± 2.8	3.0
15	$\beta$ And	M0 III	+12.6 ± 2.2	5.7

Targets of all luminosity classes from dwarfs to supergiants have shown the presence of the magnetic fields. The selected results of magnetic field measurements on stars of I-II-III luminosity classes, when a significant field was recorded, are presented in the Table 1. For stars with the repeated magnetic field detection, the values with the highest  $B_e/\sigma$  ratio are presented. The sign “5)” for the supergiant  $\epsilon$  Gem indicates that the field exceeding  $3\sigma$  was detected for 5 dates. The sign “2)” means that the field was detected for 2 dates. A more detailed review of the results of Crimean observations of the magnetic fields is given in [Plachinda and Butkovskaya \(2020\)](#).

In the spectropolarimetric survey of [Plachinda \(2005\)](#), observations of four supergiants  $\beta$  Aqr (G0 Ib),  $\alpha$  Aqr (G2 Ib),  $\epsilon$  Gem (G8 Ib), and  $\epsilon$  Peg (K2 Ib) were carried out. The statistically reliable values of the magnetic field were obtained twice for  $\epsilon$  Peg. The magnetic field on the supergiant  $\epsilon$  Gem was measured over 14 nights from 1994 to 2002. The significant field in the range from -10 to +38 G was recorded over 5 nights, whereas the relict field of supergiants should be several orders below 1 gauss because of the large radius of the star  $140 R_\odot$ . Therefore, the fact that the field on the surface

of convective supergiant can reach ten gauss is a confident evidence of the generation of the magnetic field by dynamo processes in the convective envelope.

## 2.2 T Tauri, RS CVn, LQ Hydrae and M dwarfs

Strong, up to several kilogauss, magnetic fields were measured in the accretion column of young T Tauri stars (Donati et al., 1997; Johns-Krull et al., 1999a, b). It was also found that in active dwarfs of spectral type M, the magnetic field strength in spots can reach about 5 kG (Saar and Linsky, 1985; Saar, 1994; Johns-Krull and Valenty, 1996).

In the first work on the magnetic field of HR 1099 (Donati et al., 1990), according to the authors, the magnetic field on the surface of the star can reach between  $\sim 500$  G and  $\sim 1500$  G. Donati et al. (1999) presented the results of 6-year observations of the magnetic field on the RS CVn star HR 1099 ( $P_{rot} = 2.6$  days) and young dwarf LQ Hydrae ( $P_{rot} = 1.8$  days). They concluded that the generation of the magnetic field for these late-type rapid rotators is due to dynamo mechanisms operating in the entire convective envelope.

Morin et al. (2010) presented spectropolarimetric measurements on 11 fast rotating active M dwarfs. Shulyak et al. (2017) and Shulyak et al. (2019) presented the results of spectroscopic measurements of the magnetic field strength in 29 fast rotating active M dwarfs. All dwarfs showed the presence of the magnetic field exceeding 1 kG, and some of them host much stronger average magnetic fields up to 5–7 kG. To explain the obtained results, Shulyak et al. (2019) assumed two types of dynamo states that may exist in M dwarfs.

## 3 The latest results

### 3.1 Supergiants: review published in 2010

The next survey of the magnetic fields of supergiants was done by Grunhut et al. (2010). A sample of stars in this survey consisted of 33 objects including 4 stars which were observed by Plachinda (2005). A field was detected in 9 of them (see Table 2). Some of the objects for which  $B_e$  was found to be insignificant, nevertheless, show the presence of circular polarization. Figure 1 demonstrates a confidently detected Stokes V signal for  $\epsilon$  Gem which was derived using the LSD technique. However, the value of the magnetic field is close to zero  $B_e = -0.14 \pm 0.19$  G and is most likely due to the complex distribution of the magnetic field on the surface of the star.

Note the discrepancy between values of the magnetic field of  $\epsilon$  Gem in Table 1 and Table 2. In the first case the SL method was used on a small set of relatively deep spectral lines. In the second case the LSD method was used on a large set of lines with diverse intensity. It is thus possible that both methods, on average, probed different parts of the stellar atmosphere indicating a nonuniform distribution of the magnetic field on the stellar surface or with height in the atmosphere, or both. It may also be indicative of the time evolution of the magnetic field between the two dates of observations. At this point, it is not possible to answer this question and more observations are needed to confirm or rule out possible scenarios.

**Table 2.** Supergiants

N	Object	Sp	$B_e \pm \sigma$	FAP
1	$\alpha$ Lep	F0 Ib	$+0.03 \pm 0.37$	2.420E-07
2	$\alpha$ Per	F5 Iab	$+0.82 \pm 0.37$	<1E-16
3	$\eta$ Aql	F6 Iab	$-0.23 \pm 0.75$	6.985E-08
4	$\beta$ Dra	G2 Iab	$-1.16 \pm 0.25$	<1E-16
5	$\xi$ Pup	G6 Ia	$+0.24 \pm 0.28$	<1E-16
6	$\epsilon$ Gem	G8 Ib	$-0.14 \pm 0.19$	<1E-16
7	cPup	K2.5 Ib-II	$+1.10 \pm 0.39$	1.410E-06
8	32Cyg	K3 Ib+	$+1.16 \pm 0.49$	2.053E-04
9	$\lambda$ Vel	K4.5 Ib-II	$+1.72 \pm 0.33$	5.995E-15

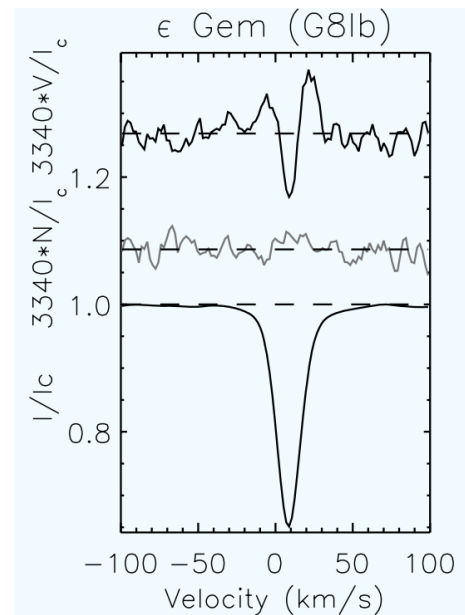


**Fig. 1.** LSD Stokes V (top), Stokes diagnostic null (middle) and Stokes I (bottom) profiles for the supergiant  $\epsilon$  Gem with the detected Stokes V signature (Grunhut et al., 2010). Profiles are vertically offset for display purposes.

### 3.2 Giants: review published in 2015

A survey of the magnetic fields of slowly rotating single convective giants was published by Aurière et al. (2015). In the sample of 48 giants selected for observations, 24 giants were characterized in the literature as strongly or moderately magnetically active. Among them, 7 objects are candidates for the presence of the strong magnetic fields that could strongly suppress convection and 17 are bright objects convenient for high-precision spectropolarimetric observations. The data were obtained with instruments ESPaDOnS (Canada-France-Hawaii Telescope (CFHT)) and Narval at the T el escope Bernard Lyot (TBL, Pic du Midi Observatory, France). The LSD method was used to calculate the longitudinal field and Stokes V profiles. The advantages and disadvantages of this approach have been widely discussed in the literature, such as, e.g., Donati et al. (1997), Donati and Landstreet (2009), Sennhauser et al. (2009), Kochukhov et al. (2010), Tkachenko et al. (2013), Plachinda (2014), Wade et al. (2016), Plachinda et al. (2019), Ram irez V elez (2020), Plachinda and Butkovskaya (2020), Plachinda et al. (2021).

The criteria for the presence of the magnetic field on the stellar surface were both the statistical significance of the longitudinal component  $B_e$  and the reliable detection of the Stokes V signals. The magnetic fields ranging from one gauss to several tens of gauss were found for 29 objects. These giants are mainly active ones with X-ray luminosity in the range  $L_x \sim 10^{29} \div 10^{31} \text{ erg s}^{-1}$ . Also, 7 giants with a weak level of activity ( $L_x \leq 10^{28} \text{ erg s}^{-1}$ ) also showed significant magnetic fields. Using the observed maximum unsigned longitudinal magnetic field,  $|B_e|_{max}$ , the following results were obtained: 3 stars have  $|B_e|_{max}$  stronger than 20 G, 5 are between 20 G and 10 G, and 21 stars have  $|B_e|_{max}$  weaker than 10 G.

As mentioned above, the LSD method assumes uniform physical conditions both on the surface of the star and with atmospheric depth. However, such uniformity is not observed in real atmospheres of stars, especially those that have convective envelopes and thus generate a number of surface structures (including active regions). The different physical conditions on the surface and with depth in different places of the atmosphere affect the formation of spectral lines. Thus, measuring the magnetic field values from spectral lines that, e.g., probe different atmospheric depths could potentially help in detecting such atmospheric structures.

To check the possible presence of the inhomogeneous physical conditions on the surface of giants, Plachinda et al. (2021) used spectropolarimetric observations of  $\epsilon$  Tau obtained at the 3.6 m CFHT telescope with the ESPaDOnS instrument over 10 nights between 2008 and 2010. Initially, a weak magnetic field of about 1.3 G was reported in Aurière et al. (2015). In Plachinda et al. (2021) we checked original spectra for instrumental effects in circular polarization and found many random outliers that could reach up to 2% in strength in all spectral orders. In the original work of Aurière et al. (2015) a full set of spectral lines, including those distorted by polarization outliers, were used to calculate the magnetic field value. In this regard, the SL technique allows to exclude from processing the spectral lines distorted by outliers. As a result, we had to exclude up to 50% of initially available spectral lines, but the measurement accuracy decreased from several tenths of gauss to two gauss on some dates (see details in Plachinda et al., 2021).

The significant value of the magnetic field was registered only on one night out of 10 observing nights:  $5.48 \pm 1.56 \text{ G}$  (Plachinda et al., 2021). It was also found that for two nights out of ten the set of the magnetic field values was nonuniform with high reliability. Therefore, Plachinda et al. (2021) concluded that the magnetic field on  $\epsilon$  Tau could be inhomogeneous on these two nights of observations.

#### 4 Magnetic field measured at different depths in the atmosphere of the giant $\delta$ CrB

In the high-precision spectropolarimetric measurements of the magnetic field in the “quiet Sun” regions, single spectral lines are usually used. Today, the extensive literature exists on the observed inhomogeneous structure of the large-scale magnetic field on the surface of the Sun. In the case of the Sun it is also well known that different lines, which are formed in different atmospheric layers, give different values of the magnetic field (see, e.g., Stenflo et al., 2013).

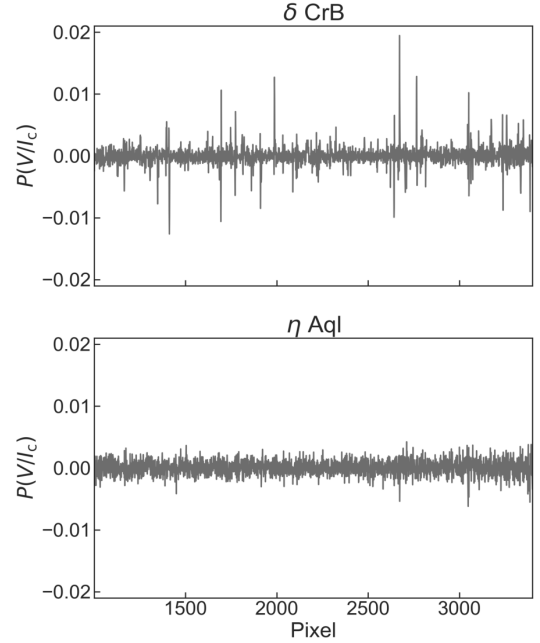


**Fig. 2.** Circular polarization in the spectrum of  $\delta$  CrB (2010-02-02) and  $\eta$  Aql (2017-08-08). The Y axis shows the Stokes V profile, and the X axis shows the pixel numbers. Edges of the spectra on blue and red sides are cut off due to the low signal-to-noise ratio. The upper panel shows the circular polarization artifacts in the spectrum. The amplitude of these polarization outliers reaches 1-2%. Circular polarization in the spectrum of  $\eta$  Aql without any outliers was taken from Plachinda et al. (2021).

To test whether the measured value of the magnetic field on giants depends on the atmospheric depth, we re-processed spectropolarimetric observations of  $\delta$  CrB (G3.5 III) from the public database of ESPaDOnS (CFHT) (6 nights). In the original article, Aurière et al. (2015) detected the magnetic field with a longitudinal component reaching 6 G.

In the observations of this star, the instrumental outliers in circular polarization were detected (see Figure 2) in all spectral orders similar to the case of  $\epsilon$  Tau described above. Therefore, we individually selected the undistorted lines similar to Plachinda et al. (2021). After that, we checked the obtained set of magnetic field measurements for uniformity. The sets of magnetic field values were found to be nonuniform with high reliability over all 6 dates. We suppose that this nonuniformity of each set tells us about the inhomogeneity of the magnetic field on the star, as we corrected the polarization spectra for instrumental effects. By analogy with the Sun, this inhomogeneity can be due to the inhomogeneity of the field both over the surface and with depth.

Here we present preliminary results of the analysis of the radial dependence of the longitudinal field strength ( $B_e$ ) in the stellar atmosphere. We estimate effective depths of the formation of spectral lines by calculation of the weighted average value of the height in the stellar atmosphere at the spectral line center. As a weighting function we used the contribution function calculated following Achmad et al. (1991). The LTE model of the  $\delta$  CrB atmosphere was calculated and the entire atmosphere was divided into 72 layers. For each spectral line we identified the layer which corresponds to the effective

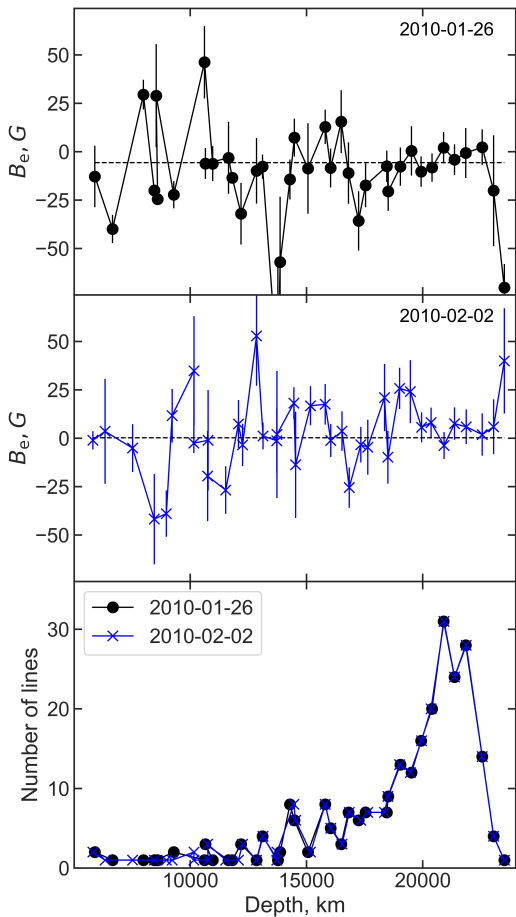


**Fig. 3.** Dependence of the field strength ( $B_e$ ) on the depth of formation of spectral lines is shown in the top panel (2010-01-26: black circles) and in the middle panel (2010-02-02: blue crosses). The bottom panel shows the number of spectral lines which were used for magnetic field measurements at different depths in the atmosphere.

depth of line formation. After that, sets of spectral lines were formed whose depths of formation were corresponding to particular atmospheric layers and the mean magnetic fields and their errors were then calculated for each layer.

The results for the two nights of observations are shown in Fig. 3. Black circles and blue crosses show the average longitudinal field for a given layer for two dates, respectively. The horizontal dashed straight lines correspond to the mean values of the field detected for these dates. The bottom panel shows the number of magnetic field measurements at different atmospheric depths. The layer 1 corresponds to the top of the atmosphere.

One can see in Fig. 3 no evidence for the depth-dependence of the longitudinal magnetic field strength. Observations on other nights showed the same result. Hence, we infer that the accuracy of these observations is probably not sufficient to detect any variation of the magnetic field with depth. We can only speculate that the magnetic field configuration on  $\delta$  CrB is likely to be inhomogeneous, which is also an argument in favor of the presence of dynamo processes in the convective envelopes of giant stars.

## 5 Conclusions

Presently, an extensive database of magnetic field observations over three decades has been accumulated for stars of all luminosity classes, both with fully and partially convective envelopes. An analysis by different authors allows us to assert that the generation of the magnetic fields in convective stars, including slowly rotating ones, occurs at all stages of evolution. These dynamo processes generate complex magnetic fields and inhomogeneous surface structures similar to active regions on the Sun. The detailed studies of the magnetic fields associated with these structures require very high-precision spectropolarimetric observations and new analysis methods that must be sensitive to different physical conditions that are expected to be present on the stellar surfaces but could not be spatially resolved in distant stars. Here we attempted to measure the large-scale magnetic fields from individual and carefully selected spectral lines in order to search for a hint of the radial variations of the magnetic field in the atmosphere of the giant  $\delta$  CrB. We detect no obvious signature for such a dependence, though we note that the distribution of our magnetic field measurements is not uniform for all 6 nights of observations, which may hint at the existence of large scale magnetic structures. More work and observations are needed to address this question in more detail.

**Acknowledgements.** Plachinda S. acknowledges the support of the Ministry of Science and Higher Education of the Russian Federation under the Grant 075-15-2020-780 (N13.1902.21.0039). Observations of the  $\delta$  CrB star were obtained at the Canada–France–Hawaii Telescope (CFHT) using ESPaDOnS. This research used the facilities of the Canadian Astronomy Data Center operated by the National Research Council of Canada with the support of the Canadian Space Agency. Shulyak D. acknowledges the financial support from the State Agency for Research of the Spanish MCIU through the “Center of Excellence Severo Ochoa” award to the Instituto de Astrofísica de Andalucía (SEV-2017-0709).

## References

- Achmad L., de Jager C., Nieuwenhuijzen H., 1991. *Astron. Astrophys.*, vol. 250, p. 445.
- Aurière M., Konstantinova-Antova R., Charbonnel C., et al., 2015. *Astron. Astrophys.*, vol. 574, p. A90.
- Borra E.F. and Vaughan A.H., 1977. *Astrophys. J.*, vol. 216, p. 462.
- Borra E.F., Edwards G., Mayor M., 1984. *Astrophys. J.*, vol. 284, p. 211.
- Butkovskaya V.V., Plachinda S.I., 2007. *Astron. Astrophys.*, vol. 469, p. 1069.
- Donati J.-F., Semel M., Rees D.E., Taylor K., Robinson R.D., 1990. *Astron. Astrophys.*, vol. 232, p. L1.
- Donati J.-F., Semel M., Carter B.D., Rees D.E., Collier Cameron A., 1997. *Mon. Not. Roy. Astron. Soc.*, vol. 291, p. 658.
- Donati J.-F., 1999. *Mon. Not. Roy. Astron. Soc.*, vol. 302, p. 457.
- Donati J.-F., Landstreet J.D., 2009. *Ann. Rev. Astron. Astrophys.*, vol. 47, p. 333.

- Grunhut J.H., Wade G.A., Hanes D.A., Alecian E., 2010. *Mon. Not. Roy. Astron. Soc.*, vol. 408, p. 2290.
- Johns-Krull C.M., Valenti J.A., 1996. *Astrophys. J.*, vol. 459, p. L95.
- Johns-Krull C.M., Valenti J.A., Hatzes A.P., Kanaan A., 1999a. *Astrophys. J.*, vol. 510, p. L41.
- Johns-Krull C.M., Valenti J.A., Koresko C., 1999b. *Astrophys. J.*, vol. 516, p. 900.
- Hubrig S., Plachinda S.I., Hunsch M., Schroder K.-P., 1994. *Astron. Astrophys.*, vol. 291, p. 890.
- Kochukhov O., Makaganiuk V., Piskunov N., 2010. *Astron. Astrophys.*, vol. 524, p. A5.
- Morin J., Donati J.-F., Petit P., et al., 2010. *Mon. Not. Roy. Astron. Soc.*, vol. 407, p. 2269.
- Plachinda S.I., Butkovskaya V.V., Pankov N.F., 2021. *Astron. Nachr.*, vol. 342, p. 607.
- Plachinda S.I., Butkovskaya V.V., 2020. *Acta Astrophys. Tau.*, vol. 1, no. 2, p. 26.
- Plachinda S., Shulyak D., Pankov N., 2019. *Astron. Astrophys. Trans.*, vol. 31, p. 323. ([arXiv:1910.01501](https://arxiv.org/abs/1910.01501)).
- Plachinda S.I., Tarasova T.N., 1999. *Astrophys. J.*, vol. 514, p. 402.
- Plachinda S.I., 2004. In Videen G., Yatskiv Ya.S., Mishchenko M.I. (Eds), *Photopolarimetry in Remote Sensing*. Kluwer Academic Publishers, p. 351.
- Plachinda S.I., 2005. *Astrophysics*, vol. 48, p. 9.
- Plachinda S.I., 2014. *Izv. Krymsk. Astrofiz. Observ.*, vol. 110, p. 17.
- Ramírez Vélez J.C., 2020. *Mon. Not. Roy. Astron. Soc.*, vol. 493, p. 1130
- Saar S.H., 1994. In Rabin D.M. et al. (Eds), *Infrared Solar Physics*, IAU Symp. No. 154. Dordrecht: Kluwer, p. 493.
- Saar S.H., Linsky J.L., 1985. *Astrophys. J.*, vol. 299, p. L47.
- Sennhauser C., Berdyugina S.V., Fluri D.M., 2009. *Astron. Astrophys.*, vol. 507, p. 1711.
- Shulyak D., Reiners A., Engeln A., Malo L., Yadav R., et al., 2017. *Nature Astronomy*, vol. 1, id. 0184.
- Shulyak D., Reiners A., Nagel E., Tal-Or L., Caballero J.A., et al., 2019. *Astron. Astrophys.*, vol. 626, p. A86.
- Stenflo J.O., Demidov M.L., Bianda M., Ramelli R., 2013. *Astron. Astrophys.*, vol. 556, p. A113. ([arXiv:1307.1117](https://arxiv.org/abs/1307.1117)).
- Tarasova T.N., 2002. *Astron. Rep.*, vol. 46, p. 474.
- Tkachenko A., Van Reeth T., Tymbal V., Aerts C., Kochukhov O., Debosscher J., 2013. *Astron. Astrophys.*, vol. 560, p. A37.
- Wade G.A., Neiner C., Alecian E., Grunhut J.H., Petit V., 2016. *Mon. Not. Roy. Astron. Soc.*, vol. 456, p. 2.